

Transport properties and origin of ferromagnetism in (Ga,Mn)As

F. Matsukura,* H. Ohno,† A. Shen, and Y. Sugawara

Laboratory for Electronic Intelligent Systems, Research Institute of Electrical Communication, Tohoku University, Sendai 980-77, Japan

(Received 19 August 1997)

Magnetotransport properties of *p*-type ferromagnetic (Ga,Mn)As, a diluted magnetic semiconductor based on III-V semiconductors, are measured and the *p*-*d* exchange between holes and Mn 3*d* spins is determined. The ferromagnetic transition temperatures calculated based on the Ruderman-Kittel-Kasuya-Yosida (RKKY) interaction using the exchange reproduce remarkably well the observed ferromagnetic transition temperatures, demonstrating that ferromagnetism of (Ga,Mn)As has its origin in the RKKY interaction mediated by holes. [S0163-1829(98)50104-X]

Interplay between cooperative phenomena and carrier transport is a source of rich solid state physics. A number of new phenomena in the transport properties of semiconductor heterostructures have been discovered in the past two decades. Only a limited number of transport studies, however, have been conducted on the cooperative phenomena in semiconductors and research in semiconductor heterostructures is virtually nonexistent. So far, conducting semiconductors that show cooperative phenomena are limited to magnetic semiconductors, such as (Eu,Gd)S (Ref. 1) and CdCr₂Se₄,² with the exception of a small band gap IV-VI-based diluted magnetic semiconductor (DMS) (Pb,Sn,Mn)Te.³ Heterostructures based on these materials are difficult to prepare; they are not easy to prepare even in bulk form. II-VI-based DMS's and their heterostructures have not been suitable for transport studies because of difficulty in doping.⁴ On the other hand, III-V-based DMS's,^{5,6} especially ferromagnetic *p*-type (Ga,Mn)As,⁷ offer an opportunity to explore various aspects of carrier transport in the presence of cooperative phenomena, since (Ga,Mn)As is conducting, can be doped to *n* type, and is compatible with GaAs-based heterostructures.⁸ In this paper, we report results of detailed magnetotransport study of ferromagnetic *p*-type (Ga,Mn)As layers ($p = 10^{18} - 10^{20} \text{ cm}^{-3}$) with Curie temperature as high as 110 K. The measurements allowed us to determine the *p*-*d* exchange between carrier spin and Mn spin J_{pd} in (Ga,Mn)As. The origin of ferromagnetism is quantitatively shown to be the Ruderman-Kittel-Kasuya-Yosida (RKKY) interaction via J_{pd} .

The (Ga,Mn)As layers were prepared by molecular-beam epitaxy (MBE) at low growth temperatures (200–300 °C) to suppress the surface segregation of Mn and formation of the MnAs second phase during growth. The 200-nm-thick (Ga_{1-x}Mn_x)As layers with Mn composition $x = 0.015 - 0.071$ were grown on an (Al_{0.9}Ga_{0.1})As buffer layer on semi-insulating GaAs (001) substrates. No intentional doping was used during growth. Six samples, which had $x = 0.015, 0.022, 0.035, 0.043, 0.053,$ and 0.071 , used in this study are hereafter referred to as samples 1–6 in order of increasing x . Details of the epitaxial growth of (Ga,Mn)As as well as its basic properties were presented elsewhere.^{7,9} In short, the lattice constant a of (Ga,Mn)As increases linearly with x following Vegard's law and a extrapolated to $x = 1$ is 0.598 nm. The maximum Mn concentration so far is 0.071, above

which formation of MnAs takes place during MBE growth even at low growth temperatures. The easy axis of magnetization is in plane due to compressive strain in the film: when the sign of strain is reversed using an appropriate buffer layer, the easy axis can be made perpendicular to the plane.¹⁰ The saturation magnetization of the samples is consistent with $S_{\text{Mn}} = 5/2$, the expected value for Mn²⁺ state.

Temperature T (2–300 K) and magnetic field B (up to 7 T, and perpendicular to the sample plane) dependence of resistivity ρ , and Hall resistivity ρ_{Hall} were measured using Hall bar geometry. Figure 1 shows the results of such measurements of sample 5. The rapid increase and saturation at low fields of ρ_{Hall} gradually become apparent as the tempera-

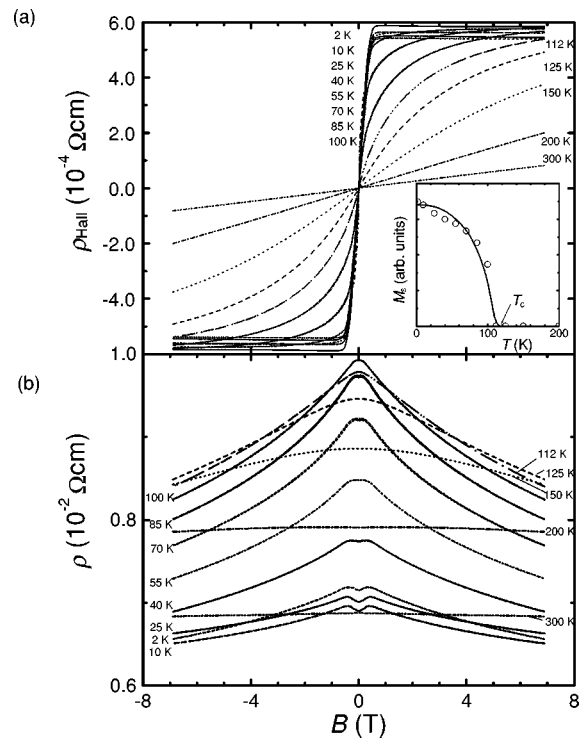


FIG. 1. Magnetic-field dependence of Hall resistivity ρ_{Hall} and resistivity ρ of (Ga,Mn)As with temperature as a parameter. Mn composition is $x = 0.053$. The inset shows the temperature dependence of the spontaneous magnetization M_s , determined from magnetotransport measurements; solid line is calculation by a mean-field theory.

ture is lowered; at low temperatures, ρ_{Hall} shows only a small linear dependence on B at high fields [not clearly seen in Fig. 1(a) due to its scale]. Negative magnetoresistance is observed in the whole temperature range of the present experiment and is most pronounced at intermediate temperatures (30–110 K). At low temperatures a small positive magnetoresistance appears at low-field region.

We first analyze ρ_{Hall} . ρ_{Hall} of magnetic materials such as (Ga,Mn)As is expressed as,

$$\rho_{\text{Hall}} = R_0 B + R_s M, \quad (1)$$

where R_0 is the ordinary Hall coefficient, R_s the anomalous Hall coefficient, and M the magnetization of the samples. From comparison between the results of magnetization and magnetotransport measurements (not shown, see Ref. 7), R_s is shown to be proportional to ρ and thus $R_s = c\rho$, where c is a constant, indicating that the skew scattering is responsible for the appearance of the anomalous Hall effect.¹¹ The contribution from the ordinary Hall effect is negligible in most of the temperature range investigated, since the slope of ρ_{Hall} at the lowest temperature under high magnetic fields (where M saturates and hence is constant) is very small [see Fig. 1(a)]. One can therefore determine M from the magnetotransport measurements alone once c in $R_s = c\rho$ is known (c is typically $1.2\text{--}1.9\text{ T}^{-1}$). The temperature dependence of the spontaneous magnetization M_s and the ferromagnetic transition temperature T_c can be determined from the field dependence of magnetization M_{Hall} obtained from magnetotransport measurements ($M_{\text{Hall}} = \rho_{\text{Hall}}/c\rho$), using an Arrott plot (where M_{Hall}^2 is plotted against B/M_{Hall}). The results are shown in the inset of Fig. 1(a). The shape of M_s - T can be described well with a simple mean-field theory using a Brillouin function with $S_{\text{Mn}} = 5/2$ as shown by the solid line in the inset. T_c of this sample was determined to be 110 K. The paramagnetic Curie temperature θ can also be determined from the temperature dependence of the inverse of the zero-field slope of M_{Hall} . A straight line characteristic of the Curie-Weiss law was obtained for all the samples (not shown), and $\theta \approx T_c$. The small linear slope of the $\rho_{\text{Hall}}-B$ curves at low temperatures ($T \leq 10$ K) under high magnetic fields ($B = 5\text{--}7$ T) allowed us to determine R_0 . The conduction type was p type for all samples and the hole concentration p of the sample shown in Fig. 1 was $1.5 \times 10^{20}\text{ cm}^{-3}$.

Figure 2 summarizes the x dependence of T_c and p . T_c is approximately proportional to x up to $x = 0.053$, above which it appears to start to decrease. The highest T_c so far obtained is 110 K. p also increases with x and peaks at $x = 0.053$. Since Mn is divalent, one might expect $p \approx [\text{Mn}]$. However p is 15% of Mn concentration $[\text{Mn}]$ at most. This may be due to compensation of Mn acceptors by deep donors such as the As antisite known to be present with high concentration in low-temperature grown GaAs.¹² The hole concentration of the samples with low x (samples 1 and 2) and high x (6) may contain appreciable error. This is because of the insulating nature of these samples as shown in Fig. 3 and the appearance of an additional paramagnetic component,¹³ both of which make accurate measurements at low T and high B difficult.

Now we turn to ρ . Figure 3 shows the temperature dependence of ρ for all the samples. As seen in Fig. 3, the samples

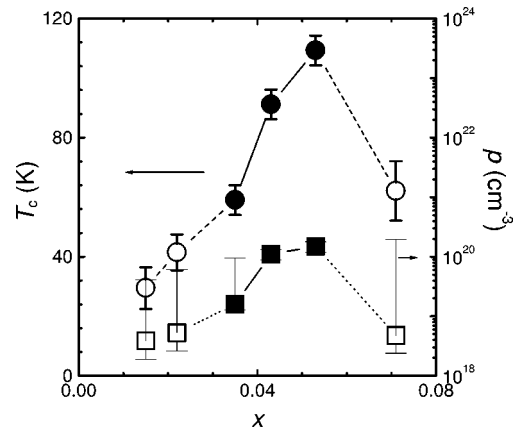


FIG. 2. Mn composition dependence of ferromagnetic transition temperature T_c and hole concentration p . Samples on the metal side of the metal insulator transition are shown by the closed symbols (see also Fig. 3).

with intermediate x (samples 3, 4, and 5) are on the metal side of the metal-insulator transition, whereas low and high x samples are on the insulator side. All the ρ - T curves showed a maximum (a hump) around T_c , which moved to higher temperature with increasing B (see the inset for sample 5). Although a hump is seen in all samples, it is somewhat obscured by the rapid increase in resistance for the insulating samples. This critical behavior of ρ is commonly observed in magnetic metals¹⁴ and magnetic semiconductors^{1,2} and is known to be due to the scattering of carriers by magnetic spin fluctuation via exchange interaction. To avoid complication arising from the localization effect, we hereafter concentrate on the behavior of the metallic samples. The nature and the mechanism of this metal-insulator transition are discussed elsewhere.¹³

The observed negative resistance in Fig. 1(b) (a metallic sample) can be understood as the reduction of scattering by aligning spins by B . Well above T_c , where there is only small spin correlation among Mn spins, one can use the spin-disorder scattering formula to describe the B dependence of

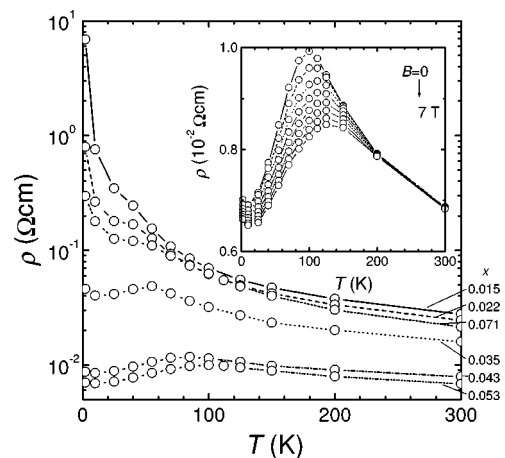


FIG. 3. Temperature dependence of ρ at zero field for $x = 0.015\text{--}0.071$. The samples with $x = 0.035\text{--}0.053$ show the metallic behavior. The inset shows the expanded view of the sample with $x = 0.053$ at around T_c with the magnetic-field dependence; other metallic samples show essentially the same critical behavior.

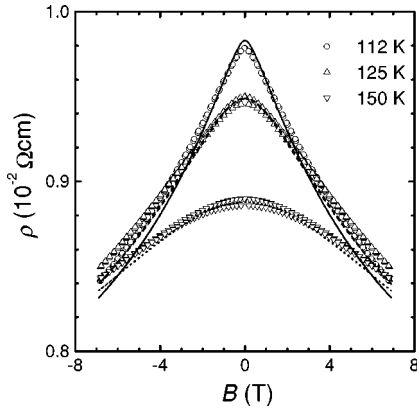


FIG. 4. Negative magnetoresistance at three different temperatures above T_c for the sample with $x=0.053$. The solid lines show fits using Eq. (3).

ρ , from which J_{pd} can be determined. For the description of the critical behavior in the temperature dependence of ρ , one needs to take into account the wave-vector-dependent susceptibility.¹

Carriers are scattered by the exchange interaction of the following form:

$$H = -J_{pd} \sum_i \delta(r - R_i) \mathbf{S}_i \cdot \mathbf{s}, \quad (2)$$

where \mathbf{S}_i is the Mn spin at site R_i and \mathbf{s} is the spin of the carrier at site r . This interaction gives rise to the following spin-disorder scattering resistivity ρ_s .

$$\rho_s = 2\pi^2 \frac{k_F}{pe^2} \frac{m^2 J_{pd}^2}{h^3} n_s [S(S+1) - \langle \mathbf{S} \rangle^2], \quad (3)$$

where k_F is Fermi wave number, e the elementary charge, m the effective mass of carrier, h Planck constant, n_s the density of Mn, $S=5/2$ the Mn spin, and $\langle \mathbf{S} \rangle$ the thermal average of \mathbf{S} .¹⁵

Figure 4 shows the result of the fit using Eq. (3) with J_{pd} as a parameter. Single value of $J_{pd} = 150 \pm 40$ eV \AA^3 not only reproduced very well the B dependence of ρ at various temperatures above T_c as shown in Fig. 4, but also reproduced the ρ - B curve of other metallic samples above T_c . For the fit, the measured p was used, assuming no temperature dependence (which is reasonable for a degenerate system). $\langle \mathbf{S} \rangle$ was calculated from $M_{\text{Hall}} = n_s g \mu_B \langle \mathbf{S} \rangle$, where $g=2$ is the Lande's g factor of Mn and μ_B the Bohr magneton. k_F was calculated from p assuming a spherical Fermi surface. A GaAs heavy-hole mass of $0.5 m_0$ (m_0 , free electron mass) was used for m .

The small positive magnetoresistance observed at low T in Fig. 1(b) is most probably caused by the rotation of spins from its original in-plane direction to the perpendicular direction. The maximum of the magnetoresistance corresponds to the ‘‘knee’’ of magnetization. This positive magnetoresistance disappears when B is applied parallel to the sample plane (not shown). The small residual negative magnetoresistance seen at higher B at low T may be attributed to the alignment of a small amount of spins that are originally canted by some local inhomogeneity.

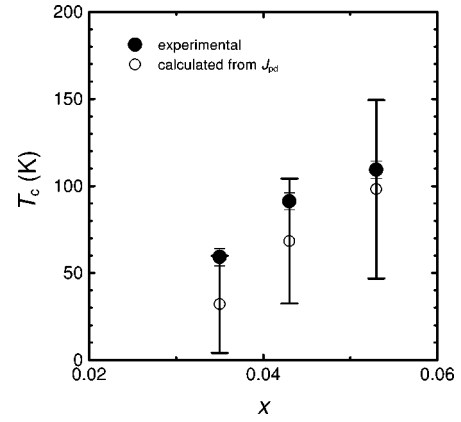


FIG. 5. Comparison between the experimental T_c (closed circles) and the calculated T_c (open circles). The error bars for the calculated T_c represent the error involved in determining exchange and carrier concentration.

Finally, we discuss the origin of ferromagnetism of (Ga,Mn)As. Since the magnetic interaction between Mn in the cation sublattice in zinc-blende structure is known to be antiferromagnetic,¹⁶ the ferromagnetic interaction responsible for the observed ferromagnetism in (Ga,Mn)As is most likely carrier induced. We examine whether the observed ferromagnetism of (Ga,Mn)As fits into the framework of the RKKY interaction mediated by carriers. The RKKY exchange Hamiltonian between the Mn spins at sites i and j is expressed by $H = -J_{ij} \mathbf{S}_i \cdot \mathbf{S}_j$, where J_{ij} is given by

$$J_{ij} = -\frac{2mk_F^4}{\pi h^2} J_{pd}^2 F(2k_F r_{ij}) \exp\left(-\frac{r_{ij}}{l}\right). \quad (4)$$

Here r_{ij} is the distance between i and j , and $F(2k_F r_{ij})$ is the ordinary RKKY oscillation term, and l is the mean free path of carriers. The term $\exp(-r_{ij}/l)$ in Eq. (4) represents the effect of a finite l following de Gennes.¹⁷ From Eq. (4), T_c is given by,

$$T_c = \frac{1}{3} x S(S+1) \sum_r z_r J_{ij}(r), \quad (5)$$

where z_r is the number of r th nearest group-III sites.

Using the values determined by experiments, including J_{pd} , one can calculate T_c for the three metallic samples using Eqs. (4) and (5), and compare them with the experimentally determined T_c . This is done in Fig. 5. As one can see the agreement is excellent. The error bars in Fig. 5 reflect the errors of J_{pd} and p . l was calculated from the carrier mobility at 10 K, which were in the range of 0.50–0.65 nm. The sign of the RKKY interaction is in effect only ferromagnetic in the present case, because the first zero of the oscillating term in Eq. (4) occurs at a much longer distance than l owing to the low carrier concentration. This gives rise to the uniform ferromagnetism that can be described by a simple mean-field theory. The quantitative consistency of the measured and calculated T_c using J_{pd} determined from the field dependence of the spin-disorder scattering clearly demonstrates that the origin of the ferromagnetic order in (Ga,Mn)As is the RKKY interaction.

It is interesting to note that $T_c/x \sim 2000$ K for (Ga,Mn)As is one of the highest induced by carriers. This is due to the large $J_{pd} = 150 \text{ eV } \text{\AA}^3$, or $N_0\beta = 3.3 \text{ eV}$ in terms of $N_0\beta$ commonly used to describe the p - d interaction in DMS's.¹⁸ In II-VI-based DMS's the typical value of $N_0\beta$ is 1 eV at most. The large $N_0\beta$ is consistent with $N_0\beta = 2.5 \text{ eV}$ reported by Szczytko *et al.*,¹⁹ who measured magnetoreflexance of excitonic interband transitions in heavily Mn-doped GaAs. It is possible that the present $N_0\beta$ is influenced by the spin-spin correlation of carriers.²⁰ It is not yet clear, however, whether or not this effect is important. Further work is needed to elucidate the origin of this large $N_0\beta$.

In conclusion, we have reported the results of magnetotransport measurements of ferromagnetic (Ga,Mn)As with Mn concentration in the range of $0.015 < x < 0.071$. The carrier-spin interaction manifested itself in the form of critical scattering at around ferromagnetic transition temperature,

which allowed us to determine the exchange of carrier-spin interaction as $J_{pd} = 150 \text{ eV } \text{\AA}^3$ ($N_0\beta = 3.3 \text{ eV}$). This value of exchange reproduced very well the experimentally obtained ferromagnetic transition temperature based on the RKKY formula. This quantitative agreement shows that the RKKY interaction is responsible for the appearance of ferromagnetism in (Ga,Mn)As.

The authors thank Professor O. Sakai of Tohoku University for useful discussions. This work was partially supported by a Grant-in-Aid for Scientific Research on Priority Area "Spin Controlled Semiconductor Nanostructures" (Grant No. 09244103) from the Ministry of Education, Science, Sports and Culture, Japan, by the "Research for the Future" Program (Grant No. JSPS-RFTF97P00202) from the Japan Society for the Promotion of Science, and by the Mitsubishi Foundation.

*Electronic address: f-matsu@riec.tohoku.ac.jp

†Electronic address: ohno@riec.tohoku.ac.jp

¹S. von Molnár and T. Kasuya, Phys. Rev. Lett. **21**, 1757 (1968).

²T. S. Aminov, K. P. Below, V. T. Kalinnikov, L. I. Koroleva, and L. N. Tovmasjan, J. Phys. (Paris) **41**, C5-155 (1980).

³T. Story, R. R. Galazka, R. B. Frankel, and P. A. Wolff, Phys. Rev. Lett. **56**, 777 (1986).

⁴This situation is rapidly changing owing to the recent advances in the doping technology of II-VI compounds. Very recently, spin dependent transport in II-VI DMS heterostructures has been reported by I. P. Smorchkova *et al.* [Phys. Rev. Lett. **78**, 3571 (1997)], and an indication of carrier induced ferromagnetism in a II-VI DMS heterostructure by A. Haury *et al.* [*ibid.* **79**, 511 (1997)].

⁵H. Munekata, H. Ohno, S. von Molnár, A. Segmüller, L. L. Chang, and L. Esaki, Phys. Rev. Lett. **63**, 1849 (1989).

⁶H. Ohno, H. Munekata, T. Penny, S. von Molnár, and L. L. Chang, Phys. Rev. Lett. **68**, 2664 (1992).

⁷H. Ohno, A. Shen, F. Matsukura, A. Oiwa, A. Endo, S. Katsumoto, and Y. Iye, Appl. Phys. Lett. **69**, 363 (1996).

⁸A. Shen, H. Ohno, F. Matsukura, Y. Sugawara, Y. Ohno, N. Akiba, and T. Kuroiwa, Jpn. J. Appl. Phys. **36**, L73 (1997).

⁹A. Shen, H. Ohno, F. Matsukura, Y. Sugawara, N. Akiba, T. Kuroiwa, A. Oiwa, A. Endo, S. Katsumoto, and Y. Iye, J. Cryst. Growth **175/176**, 1069 (1997).

¹⁰H. Ohno, F. Matsukura, A. Shen, Y. Sugawara, A. Oiwa, A. Endo, S. Katsumoto, and Y. Iye, in the *Proceedings of the 23rd International Conference on the Physics of Semiconductors*, Vol. 405 edited by M. Scheffler and R. Zimmerman (World Scientific, Singapore, 1996).

¹¹C. M. Hurd, in *The Hall Effect and Its Applications*, edited by C. L. Chien and C. W. Westgate (Plenum, New York, 1980), pp. 43-51.

¹²D. C. Look, J. Appl. Phys. **70**, 3148 (1991).

¹³A. Oiwa, S. Katsumoto, A. Endo, M. Hirasawa, Y. Iye, H. Ohno, F. Matsukura, A. Shen, and Y. Sugawara, Solid State Commun. **103**, 209 (1997).

¹⁴R. J. Weiss and A. S. Marotta, J. Phys. Chem. Solids **9**, 302 (1959).

¹⁵T. Kasuya, Prog. Theor. Phys. **16**, 45 (1956).

¹⁶S. von Molnár, H. Munekata, H. Ohno, and L. L. Chang, J. Magn. Magn. Mater. **93**, 356 (1991).

¹⁷P. J. de Gennes, J. Phys. Radium **23**, 630 (1962).

¹⁸J. A. Gaj, in *Semiconductor and Semimetals*, edited by J. K. Furdyna and J. Kossut (Academic, New York, 1988), Vol. 25.

¹⁹J. Szczytko, W. Mac, A. Stachow, A. Twardowski, P. Becla, and J. Tworzydło, Solid State Commun. **99**, 927 (1996).

²⁰B. L. Al'tshuler and A. G. Aronov, Zh. Eksp. Teor. Fiz. **38**, 153 (1983) [JETP Lett. **16**, 45 (1956)].